Photo-Induced Shrinking of Aqueous Glycine Aerosol Droplets

Shinnosuke Ishizuka,[a,b,c ‡, *] Oliver Reich,[a, ‡] Grégory David,[a] and Ruth Signorell[a]*

[a] Laboratory of Physical Chemistry, ETH Zurich, Vladimir-Prelog-Weg 2, CH-8093, Zurich, Switzerland

[b] Institute of Advanced Research, Nagoya University, Nagoya 046-8601, Japan

[c] Institute of Space-Earth Environmental Research, Nagoya University, Nagoya 046-8601, Japan

ABSTRACT: Due to their small size, micrometer and submicron sized solution droplets can respond differently to physical and chemical processes compared with extended bulk material. Using optically trapped micrometer sized aqueous glycine droplets, we demonstrate a photo-induced degradation of glycine upon irradiation with visible light, even though molecular glycine does not absorb light in the near UV/vis range to any significant extent. This reaction is observed as photo-induced shrinking of the droplet, which we characterize by analyzing the elastic light scattering and the Raman spectrum of the droplet over the course of the reaction. We find the volume to shrink with a constant rate over the major part of the shrinking process. This indicates the presence of a rate limiting photo-catalyst, which we attribute to mesoscopic glycine clusters in the droplet solution. Our findings relate to previous reports about enhanced absorption and fluorescence rates of amino acid solutions. However, to the best of our knowledge, this is the first experimental evidence of a photochemical pathway facilitated by mesoscopic clusters. Light interaction with such mesoscopic photoactive molecular aggregates might be more important for aerosol photochemistry than previously anticipated.

* rsignorell@ethz.ch, ishizuka.shinnosuke.a3@f.mail.nagoya-u.ac.jp

‡ S.I. and O.R. contributed equally to this work.

1. INTRODUCTION

Aerosols, dispersions of solid and liquid particles in a gas, are ubiquitous in Earth's atmosphere and as such play an important role for many atmospheric processes (Boucher et al., 2013; PöSchl and Shiraiwa, 2015). Size, chemical composition, viscosity and thermodynamic phase of aerosol particles respond to their environment including the surrounding gas species, temperature, humidity (Bones et al., 2012; Zieger et al., 2017; Tang et al., 1997; Swietlicki et al., 2008) and light irradiation (PöSchl and Shiraiwa, 2015; Cremer et al., 2016; Walser et al., 2007; Corral Arroyo et al., 2022). Particular attention has been paid to their chemistry distinct from that in the bulk, a phenomenon possibly arising from high surface to volume ratio of aerosol particles and the accessibility to highly supersaturated states (Altaf et al., 2016; Kucinski et al., 2019; Bzdek and Reid, 2017). Various chemical reactions have been shown to be accelerated in microdroplets (Cremer et al., 2016; Lee et al., 2015; Girod et al., 2011), with some reactions being exclusive to the droplet phase (Lee et al., 2019). These unique reactors can act as medium for the birth, growth and degradation of atmospherically relevant particles (Ruiz-Lopez et al., 2020), and be utilized for organic synthesis (Bain et al., 2017). Chemical processes in prebiotic aerosols have also been proposed as potential mechanisms for the origin of life (Tervahattu et al., 2004). However, molecular processes leading to the anomalous chemistry in micrometer and submicron aerosol particles are still largely unknown. Although some processes may be ascribed to the discontinuous and asymmetric intermolecular interactions at the particle surface (Ruiz-Lopez et al., 2020), the microphysical origins behind many of the aforementioned particle specific phenomena are still not adequately explored.

Glycine is an amino acid that acts as precursor to proteins and fulfills a number of other biological functions (Arnstein, 1954; Hall, 1998; Jackson, 1991). With its small size and simple structure, glycine often serves as a proxy for other amino acids and physiologically relevant molecules, and as such has been studied extensively in the past. It is generally accepted that molecular glycine does not absorb light in the near UV/vis range, similar to other amino acids (Bhat and Dharmaprakash, 2002). However, it has been shown that their optical properties change when glycine molecules arrange themselves into mesoscopic clusters by forming hydrogen bond networks (Terpugov et al., 2021). Furthermore, these formations respond to light irradiation in non-trivial ways which can be exploited to induce long range order inside the glycine solution (Alexander and Camp, 2019; Sugiyama et al., 2012; Zaccaro et al., 2001; Garetz et al., 2002; Urquidi et al., 2022) on a scale of up to millimeters (Yuyama et al., 2010). While these interactions have the potential to change the optical properties of glycine ensembles significantly and to enable new photochemical reaction pathways, there has been little experimental evidence for such reactions so far.

In this work, we study the response of aqueous glycine droplets to irradiation by visible light. We observe the shrinking of optically trapped micrometer sized glycine droplets, which can be unambiguously attributed to the exposure to the trapping laser with wavelength 532 nm. To the best of our knowledge, this interaction has not been reported before. We characterize it here with particular focus on the shrinking rate and its dependence on the

light intensity. To explain our results, we discuss possible reaction schemes based on the available experimental data. Although further data is needed to elucidate the exact photochemical pathways of the observed reaction, these findings demonstrate the existence of a photochemical reaction for molecules which previously have been considered photochemically inert at visible wavelengths.

2. METHODS

Dual beam optical traps are widely used to confine and isolate single particles (Ashkin, 1997; Gong et al., 2018; Čižmár et al., 2005; Esat et al., 2018; Reich et al., 2020). The counter-propagating tweezers (CPT) setup for trapping aqueous glycine droplets is shown in Fig. 1 and consists of a continuous green laser beam (Novanta Photonics Opus 532 6W), which is expanded and then split into two beams of equal power. These two beams are aligned counter-propagating on a single axis and focused into the trapping cell, where a single droplet is trapped between the two focii.

The droplets are generated from 1.0 M or 2.0 M aqueous solutions of glycine (purity 100%, HPLC certificate, Sigma-Aldrich G7126) using a commercial atomizer (TSI 3076) with pressurized, humidified nitrogen gas (purity 5.0). We performed additional elementary and HPLC analyses of the glycine and the glycine solutions. The results showed no indication of any trace impurities absorbing in the visible range. On this basis, we conclude that our samples do not contain any contaminants that could act as photosensitizer for photochemical reactions (see below). A system of copper tubings directs the spray of particles into the trapping cell, where the droplets agglomerate at the designated trapping position. The humidification of the nitrogen flow is necessary to ensure that the droplets reach the trapping position in the liquid state. The trapping cell is filled with nitrogen gas (purity 5.0) and a steady nitrogen flow formed by combining wet and dry nitrogen with adjustable flow ratios is used to control the relative humidity (RH) in the cell. For the experiments reported here, the RH is set at 77 ± 3 % well above the efflorescence RH of glycine at approximately 55 % (Chan et al., 2005). At this RH, the droplet solution is supersaturated with an estimated glycine concentration of 60 % in mass (Chan et al., 2005), corresponding to approximately 5 M. Temperature and RH inside the trapping cell are monitored by a sensor (Sensirion SHT35) placed a few millimeters away from the trapping position. When the agglomerated particle reaches a size of approximately 2-3μm in radius, the remainder of the droplets in the cell are flushed out with nitrogen for 20-30 minutes to ensure that only the trapped droplet remains in the cell. After flushing, the power of the trapping laser is kept constant until the end of the measurement.

The particle shrinking is monitored by imaging the polarization resolved two-dimensional angular optical scattering (polarization resolved TAOS) of the particle (Parmentier et al., 2022), as shown in Fig. 2. The TAOS image is obtained by collecting the elastically scattered light of the trapping beams under a scattering angle of $90 \pm 24°$ with an objective (Mitutoyo 20x NA 0.42). The parallel and perpendicular polarization components with respect to the scattering plane (TAOS PPol and TAOS SPol) are separated using a polarization beam splitter and recorded with separate CMOS cameras (Thorlabs DCC1545M). The scattering intensity for each polarization is calculated from the average of the respective TAOS image and recorded over time. At specific times, the shrinking spherical particle reaches a size at which it is in resonance with the light of the trapping beams, which corresponds to a Mie resonance (Bohren and Huffman, 2008). From the comparison of the recorded evolution of the polarization resolved scattering intensity to simulations using Mie theory, the size of the particle can be determined at the specific

4

79   times. Fig. 3 shows an example of such a TAOS analysis. The values of the size at the discrete points in time,

80   obtained from the times where the particles experience a Mie resonance, can then be interpolated with high accu-

81   racy to obtain the full size evolution of the particle over the course of the measurement.

82

83   The molecular composition of the particle is monitored by continuous recording of Raman spectra (David et al.,

84   2020) during the shrinking process. To this end, the light scattered by the particle is collected under a scattering

85   angle of $90 \pm 24°$ by a second objective and fiber coupled into a low noise, high sensitivity spectrograph (Andor

86   KY-328i-A). The inelastically scattered light is analyzed in the range 540-680 nm which corresponds to Raman

87   shifts of 280-4100 cm^{-1}. This range contains in particular the O-H symmetric stretching mode of water (v_2-H_2O,

88   2700-3750 cm^{-1}) as well as several vibrational modes of glycine, which we exploit for the characterization of the

89   molecular composition (see later data for an example).

90

91   **3. RESULTS AND DISCUSSION**

92   The shrinking of the aqueous glycine droplets over time is shown in Fig. 4 for three representative examples. The

93   droplets are trapped using different laser powers, which affects the rate at which their volume is decreasing. For

94   all laser powers, the volume is observed to shrink linearly with time over a large portion of the shrinking process.

95   After a certain point ('point of acceleration'), when the droplet has lost 60 – 80 % of its volume, the shrinking

96   suddenly accelerates, only to continue again approximately linearly with time, albeit at a higher rate.

97

98   To quantify the dependence of the shrinking rate on the light intensity incident on the particle, a linear fit is

99   performed on the data before and after the point of acceleration. Since between different experiments, the align-

100   ment of the optical trap, and hence the focusing of the laser light on the particle, is subject to temporal mechanical

101   drifts, the nominal laser power used for trapping of the droplets is not an optimal indicator for the incident inten-

102   sity. Instead, we use the intensity of the scattered light as a measure that is proportional to the incident light

103   intensity. The intensity of the scattered light is obtained from the average signal of the TAOS PPol and SPol

104   images during the time of the droplet shrinking. To ensure consistency between the different experiments, the

105   average of the light intensity is taken over the same volume interval of [65.4, 51.0] μm^3 (radius [2.5, 2.1] μm) for

106   all droplets. This interval corresponds to the interval for which we obtained data for most droplets. Fig. 5 shows

107   the resulting initial shrinking rates as function of light intensity. The shrinking rate is observed to be proportional

108   to the light intensity, confirming that the shrinking is induced by the trapping laser at a wavelength of 532 nm.

109

110   To gain further insight into the shrinking mechanism, we analyze the evolution of the Raman spectra over the

111   course of the shrinking process. A representative example of such an evolution is shown in Fig. 6. For Raman

112   spectra of single spherical particles, so called morphology dependent resonances, or whispering gallery modes

113   (WGMs) (Oraevsky, 2002), are superimposed on the molecular signals. To separate the WGMs from the molecular

114 signal of interest, the Raman spectra are normalized and stacked in chronological order from left to right, as shown

115 in Fig. 6a. The WGMs show up as a manifold of thin slanted lines bending towards lower wavenumbers with

116 increasing time as the droplet shrinks. Molecular band positions on the other hand are independent of particle

117 size, and are identified as horizontal lines in the evolution of the Raman spectra.

118

119 From Fig. 6a it is evident that the molecular Raman signal remains qualitatively the same, indicating that no

120 significant change in the molecular composition takes place in the droplet over the course of the shrinking process.

121 This behavior is observed for all investigated droplets. Since the particle loses the major part of its volume during

122 the shrinking, this implies that glycine is removed from the droplet as a consequence of chemical reaction (*vide*

123 *infra*). As the water vapor pressure of the droplet is given by the surrounding RH of 77 % and therefore has to

124 remain constant, the removal of glycine from the droplet must be accompanied by the evaporation of water in

125 order to maintain the equilibrium glycine concentration. A quantitative analysis of the Raman spectrum (Fig. 6b)

126 reveals that the spectral intensity of glycine modes with respect to the O-H stretching mode of water remains

127 constant, confirming a constant concentration of glycine molecules during the shrinking process. The measure-

128 ment ends when the particle becomes too small for stable trapping, and therefore leaves the optical trap.

129

130 Aqueous droplets which contain a stable non-volatile solute do not shrink over time when they are optically

131 trapped (see Supplementary Section S1 for an example). The observation of droplet shrinking in the case of dis-

132 solved glycine proves that glycine does not remain stable inside the droplet solution. Furthermore, the linear

133 dependence of the shrinking rate on the light intensity (Fig. 5) proves that the observed shrinking is induced by

134 the laser light. In particular, the volume shrinking rate increases from 0.18 to 2.25 μm^3 h^{-1} when the light intensity

135 is increased by the same relative amount, thus spanning over one order of magnitude. This observation is intri-

136 guing as aqueous glycine is not known to absorb light in the visible range, similar to other amino acids (Bhat and

137 Dharmaprakash, 2002). In addition, the linear dependence between shrinking rate and light intensity rules out the

138 possibility of multiphoton absorption, which might otherwise populate energetically excited states of glycine to

139 induce chemical reactions. The fact that the observed shrinking is driven by the incident light indicates a photo-

140 chemical reaction or photothermal processes occurring in the aqueous glycine droplet. As is shown in the follow-

141 ing however, photothermal processes can be ruled out by our experimental data.

142

143 The observation of a constant shrinking rate over a large portion of the experiments (Fig. 4) provides another

144 important piece of information, as this allows us to rule out some of the possible shrinking mechanisms. For

145 instance, assuming some residual absorption of light at 532 nm by the droplet solution, one might argue that the

146 shrinking is a consequence of enhanced evaporation due to the droplet heating by the laser. The evaporation of

147 glycine from the droplet can be approximated by the Hertz-Knudsen equation:

$$\frac{dN}{dt} = S \cdot \frac{\alpha p}{\sqrt{2\pi MRT}} \tag{1}$$

148

149   where $\frac{dN}{dt}$ is the molar evaporation rate of glycine, S is the droplet's surface, p is the partial pressure and M is the

150   molar mass of glycine, R the gas constant, T the temperature and α a heuristic sticking coefficient with values

151   between 0 and 1. It is evident from Eq. (1) that the rate of shrinking by evaporation should scale with the surface

152   area of the droplet, and that in this case a deceleration of the shrinking should be observed over time, contrary to

153   the experimental data. Moreover, any heating by laser light absorption would at most lead to a very small temper-

154   ature rise due to the efficient cooling by the surrounding gas (see Supplementary Section S2 for an upper estimate

155   of the temperature increase). In addition to these arguments, if evaporation were significant, some evaporation

156   should still be observable even at low light intensity, where the heating of the droplet is negligible and hence any

157   deviations form room temperature can be neglected. As seen from Fig. 5 however, there is no shrinking observable

158   for low light intensities. We can therefore rule out evaporation as the dominant shrinking mechanism.

160   The observation of a constant shrinking rate also excludes photochemical reactions in which molecular glycine

161   directly absorbs photons:

$$Gly(aq) + h\nu \rightarrow P(aq) \rightarrow P(g), \tag{2}$$
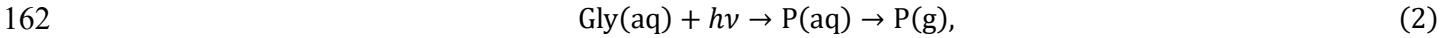
163   where Gly(aq) is a solvated glycine molecule, $h\nu$ is the energy of the incoming photon and P is the reaction prod-

164   uct that is removed from the droplet (aq) into the surrounding gas phase (g) afterwards. As mentioned above.

165   molecular glycine is considered non-absorbing at 532 nm. However, if we nevertheless assume that molecular

166   glycine could be very weakly absorbing as in Eq. (2), the photon density inside the droplet would be constant over

167   the course of the photochemical reaction. Earlier studies (Parmentier et al., 2021; Corral Arroyo et al., 2022) show

168   that no significant size dependence of the optical confinement is observed for weakly absorbing particles in the

169   micrometer- and submicrometer-size ranges. Hence, the first step in Eq. (2) would be pseudo-first order, for which

170   the reaction rate is proportional to the concentration of glycine molecules in the droplet. Therefore, one would

171   expect a decrease in the observed shrinking rate over time, which contradicts the experimental observation.

173   The examples above illustrate that any mechanism, in which glycine molecules directly absorb incoming photons,

174   cannot explain the constant shrinking rates. This implies that a more intricate reaction must take place in the

175   droplet. We suggest the following simplified scheme with an additional reaction partner M:

$$M + h\nu \rightarrow M^* \tag{3}$$

$$M^* + Gly \rightarrow M + P \tag{4}$$
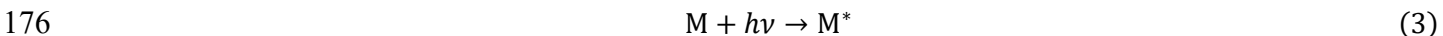
178   where M^* denotes a photoexcited state of M, and P is the reaction product of glycine in the presence of this pho-

179   toexited species. This scheme represents a mediated reaction in which the reaction partner M is activated by light

180   absorption, and then reacts with glycine and returns back to the ground state. M shows the characteristics of a

181   photosensitizer (Corral Arroyo et al., 2018; George et al., 2015; Wang et al., 2020; Rapf and Vaida, 2016), which

182   is not consumed during the reaction, and therefore the amount of M remains constant in the droplet. We further

183   assume that the light absorption of the photosensitizer M is the rate limiting step, i.e., that Eq. (3) proceeds much

184   slower than Eq. (4). This is equivalent to requiring that M is only weakly absorbing, or that the concentration of

185   M in the droplet is low. Since the amount of M in the rate limiting step (Eq. (3)) remains constant during the

186   shrinking process, so does M^* (quasistationary), resulting in a constant rate of degradation of Gly (Eq. (4)). As-

187   suming that the absolute concentration of M is much smaller than that of Gly at all times, and therefore has no

188   relevant effect on the equilibrium water vapor pressure of the droplet, the volume shrinking rate is predicted to be

189   constant in accordance with the experimental data.

190

191   Although the proposed mechanism in Eq. (3) and (4) concurs with the observed constant shrinking rates, it does

192   not yet specify the nature of the photosensitizer and its reaction with glycine. We first discuss potential candidates

193   for the photosensitizer. Contamination during the preparation of the different aqueous glycine solutions used in

194   this study was minimized by using pure substances (glycine purity $\geq$ 99 %, water resistivity 18.2 M$\Omega\cdot$s). No

195   correlation between the shrinking rates in Fig. 5 and the age of the solution at the time of the measurements was

196   observed, which indicates that there is no accumulation of photoactive contaminants in the solution after the

197   preparation. We therefore argue that contamination is not the origin of the photosensitizer.

198

199   It is evident from the previous discussion that the photosensitizer must possess an absorption band at 532 nm,

200   which is not the case for single solvated glycine molecules. The optical properties of molecules may change

201   however when forming intermolecular bonds, e.g. leading to an enhancement of the absorption and fluorescence

202   in the case of protein aggregates (Homchaudhuri and Swaminathan, 2004; Shukla et al., 2004; Chan et al., 2013;

203   Pinotsi et al., 2013) and amino acid clusters (Chen et al., 2018). For glycine solutions in particular, observations

204   of light absorption in the near UV/vis range have been attributed to the presence of mesoscopic clusters (Jawor-

205   Baczynska et al., 2013; Zimbitas et al., 2019), specifically due to the formation of hydrogen bonds between indi-

206   vidual molecules (Terpugov et al., 2021).

207

208   Mesoscopic clusters occur naturally in both undersaturated and supersaturated glycine solutions, though a kinetic

209   barrier may have to be overcome for their formation (Jawor-Baczynska et al., 2013).). A similar barrier needs to

210   be overcome to dissolve these clusters. Hence the clusters can remain kinetically stable even if the number of

211   glycine monomers decreases. The average size of the mesoscopic clusters, typically of the order of 100 nm for

212   bulk solutions, depends not only on the monomer concentration but also on the history of the sample, indicating

213   that the clusters do not necessarily remain in thermodynamic equilibrium after formation (Jawor-Baczynska et

214   al., 2013). Based on these observations, we propose that the photo-induced droplet shrinking is mediated by light

215   absorption of mesoclusters in the glycine solution. These mesoclusters remain kinetically stable during the droplet

216   shrinking, despite the decrease of the absolute number of glycine monomers (i. e. constant glycine monomer

217   concentration). Hence, these clusters act as stable photosensitizers inside the droplets, in accordance with the

218   observed constant shrinking rate. The observation of a constant initial shrinking rate thus allows us to narrow

219   down the possible reaction mechanisms at work in the droplets. Alternative schemes might be conceivable, such

220 as the existence of several reaction partners for glycine. However, there is no further experimental evidence in
221 favor of more complex alternatives to the simple mechanism proposed (Eq. (3) and (4)). Furthermore, as pointed
222 out above, mesoscopic glycine clusters match the requisite characteristics of the proposed photosensitizer, and are
223 therefore likely candidates. To pursue the argument, let us further discuss the role of the mesoscopic clusters in
224 the observed acceleration of the droplet shrinking.

225

226 The acceleration of the droplet shrinking proceeds relatively promptly at the point of acceleration when the par-
227 ticle has lost a typical amount of 75 % of its volume (Fig. 4). Assuming that the total number of mesoclusters
228 remains approximately constant (M in Eqs.(3) and (4)), their concentration has increased by an approximate factor
229 of 4 at this point. The sudden nature of the shrinking acceleration hints at a phase transition inside the particle. In
230 particular, the increase in nanocluster concentration may trigger the separation of a dense cluster phase inside the
231 droplets as part of a liquid-liquid phase transition. While a definite conclusion has to await more detailed micro-
232 scopic investigations, we present the following arguments in favor of this explanation. Mesoscopic clusters in
233 aqueous solutions are known to interact with focused light irradiation by assembling in the focal point of the light
234 beam due to the optical force that acts on the individual clusters (Sugiyama et al., 2012). This mechanism is the
235 basis of laser-induced phase transitions(Alexander and Camp, 2019), in the particular case of glycine both for
236 liquid-liquid phase separation (Sugiyama et al., 2012; Yuyama et al., 2010) and solid crystal nucleation (Sugiyama
237 et al., 2012; Alexander and Camp, 2019; Yuyama et al., 2010; Zaccaro et al., 2001; Garetz et al., 2002). It should
238 be noted at this point that the spot size in the focus of our optical trap is slightly larger (5 μm) than the typical
239 droplet size, and that therefore, it might appear unlikely that the electromagnetic field gradient is strong enough
240 to induce cluster aggregation in our case. However, micrometer sized droplets exhibit a large variance in the
241 spatial distribution of the internal light field, owing to the nanofocusing effect (Cremer et al., 2016; Corral Arroyo
242 et al., 2022), which can provide the field gradients necessary for aggregation. If in the case of our trapped droplets,
243 the acceleration is due to a phase transition, it would likely be assisted by the light irradiance. One would therefore
244 expect a dependence of the observed shrinking acceleration on the incident light intensity. Fig. 7 shows the meas-
245 ured acceleration ratio, that is, the ratio between the shrinking rate after to before the point of acceleration, as a
246 function of light intensity. From this data it is evident that the ratio increases with higher light intensity, which
247 agrees with our explanation of a light-induced phase transition. Since in this scheme, the clusters are expected to
248 aggregate in the regions of high light intensity after reaching a critical concentration, this would lead to a larger
249 absorption rate and thus a larger subsequent reaction rate, in agreement with the observation. Further studies will
250 be necessary to provide conclusive evidence for this explanation.

251

252 More data will also be required to understand the specifics of the interaction between the photosensitizer and the
253 solvated glycine molecules in Eq. (4). Here, we can only provide a qualitative discussion based on the available
254 data. The Raman spectra (Fig. 6) show no detectable change in the molecular composition, even after the droplet
255 has lost the major part of its volume during the shrinking process. Since this observation rules out the accumula-
256 tion of reaction products in the droplets over time, the reaction products must be small, volatile compounds that

257 quickly evaporate into the surrounding gas phase. Known degradation mechanisms of glycine and other amino
258 acids in aqueous solution proceed via reaction with radical species, in particular solvated electrons e_{solv}^- and hy-
259 droxyl $^{\bullet}$OH radicals (Moenig et al., 1985; Garrison, 1964, 1972), which form as part of a photosensitized reaction
260 with chromophoric organic matter in water (Lundeen et al., 2014; Sun et al., 2018; Mopper and Zika, 1987).
261 Currently, our data does not allow us to distinguish between different degradation pathways.

262

263 **4. CONCLUSIONS**

264 We have demonstrated that single micrometer sized aqueous glycine droplets respond to the illumination with
265 laser light of 532 nm by shrinking, despite the fact that molecular glycine does not absorb in the near UV/vis
266 range. Most remarkably, the volume shrinking rate remained constant over the major part of the shrinking process.
267 This indicates a photo-induced decay of glycine molecules in the presence of a rate limiting catalyst, or photosen-
268 sitizer, and the subsequent evaporation of small, volatile reaction products. Based on the available literature data,
269 we propose that intrinsic mesoscopic clusters of glycine molecules formed by hydrogen bonding in the aqueous
270 solution are the most plausible candidates for this photosensitizer. The presence of mesoscopic glycine clusters
271 would also explain the sudden acceleration of the shrinking rate occurring at a volume loss of ~75 %. Because of
272 its dependence on the light intensity, we attribute this sudden rate change to arise from the interaction of the
273 mesoclusters with the incident light, possibly initiating a light-induced phase transition.

274

275 This study provides yet another example of the non-trivial interactions of light with aqueous glycine solutions
276 (Alexander and Camp, 2019; Sugiyama et al., 2012; Zaccaro et al., 2001; Garetz et al., 2002; Yuyama et al., 2010),
277 which facilitate previously undiscovered reaction pathways - interactions that are likely not exclusive to glycine.
278 Light harvesting by and light interaction with such mesoscopic photosensitizers in aerosol droplets might also
279 have played a role in the formation of more complex organic molecules under prebiotic conditions. Further in-
280 vestigations are needed to shed light on the specifics of the observed phenomena, and to yield new insight into
281 the underlying reaction mechanisms, which remain elusive in part. Studying solutions in micrometer sized drop-
282 lets (attoliter volumes) using high laser powers offers the advantage of much higher sensitivity to photo-induced
283 reactions than typically achievable with bulk solutions.

284

285 **Data availability**

286 The data that support our findings are deposited on the ETH Research Collection, DOI: 10.3929/ethz-b-
287 000607208.

288

289 **Author contribution**

290 SI conceived the project, and carried out the experiments together with OR and contributions from GD. SI, OR
291 and GD performed the data analysis. The project was supervised by RS. All authors discussed and evaluated the

10

292 result. SI and OR prepared the manuscript draft with contributions from all authors. OR and GD revised the
293 draft during the review stage with contributions from all authors. RS edited the final manuscript.
294

295 **Competing interests**
296 The authors declare that they have no conflict of interest.

297 **Acknowledgements**

304
305

References

Alexander, A. J. and Camp, P. J.: Non-photochemical laser-induced nucleation, The Journal of chemical physics, 150, 040901, 2019.

Altaf, M. B., Zuend, A., and Freedman, M. A.: Role of nucleation mechanism on the size dependent morphology of organic aerosol, Chem. Commun., 52, 9220-9223, 2016.

Arnstein, H.: The metabolism of glycine, in: Adv. Protein Chem., Elsevier, 1-91, 1954.

Ashkin, A.: Optical trapping and manipulation of neutral particles using lasers, Proceedings of the National Academy of Sciences, 94, 4853-4860, 1997.

Bain, R. M., Sathyamoorthi, S., and Zare, R. N.: ″On‐droplet″ chemistry: the cycloaddition of diethyl azodicarboxylate and quadricyclane, Angew. Chem., 129, 15279-15283, 2017.

Bhat, M. N. and Dharmaprakash, S.: Growth of nonlinear optical γ-glycine crystals, J. Cryst. Growth, 236, 376-380, 2002.

Bohren, C. F. and Huffman, D. R.: Absorption and scattering of light by small particles, John Wiley & Sons2008.

Bones, D. L., Reid, J. P., Lienhard, D. M., and Krieger, U. K.: Comparing the mechanism of water condensation and evaporation in glassy aerosol, Proceedings of the National Academy of Sciences, 109, 11613-11618, 2012.

Boucher, O., Randall, D., Artaxo, P., Bretherton, C., Feingold, G., Forster, P., Kerminen, V.-M., Kondo, Y., Liao, H., and Lohmann, U.: Clouds and aerosols, in: Climate change 2013: the physical science basis. Contribution of Working Group I to the Fifth Assessment Report of the Intergovernmental Panel on Climate Change, Cambridge University Press, 571-657, 2013.

Bzdek, B. R. and Reid, J. P.: Perspective: Aerosol microphysics: From molecules to the chemical physics of aerosols, The Journal of Chemical Physics, 147, 220901, 2017.

Chan, F. T., Schierle, G. S. K., Kumita, J. R., Bertoncini, C. W., Dobson, C. M., and Kaminski, C. F.: Protein amyloids develop an intrinsic fluorescence signature during aggregation, Analyst, 138, 2156-2162, 2013.

Chan, M. N., Choi, M. Y., Ng, N. L., and Chan, C. K.: Hygroscopicity of water-soluble organic compounds in atmospheric aerosols: Amino acids and biomass burning derived organic species, Environ. Sci. Technol., 39, 1555-1562, 2005.

Chen, X., Luo, W., Ma, H., Peng, Q., Yuan, W. Z., and Zhang, Y.: Prevalent intrinsic emission from nonaromatic amino acids and poly (amino acids), Science China Chemistry, 61, 351-359, 2018.

Čižmár, T., Garcés-Chávez, V., Dholakia, K., and Zemánek, P.: Optical conveyor belt for delivery of submicron objects, Appl. Phys. Lett., 86, 174101, 2005.

Corral Arroyo, P., David, G., Alpert, P. A., Parmentier, E. A., Ammann, M., and Signorell, R.: Amplification of light within aerosol particles accelerates in-particle photochemistry, Science, 376, 293-296, 2022.

Corral Arroyo, P., Bartels-Rausch, T., Alpert, P. A., Dumas, S. p., Perrier, S. b., George, C., and Ammann, M.: Particle-phase photosensitized radical production and aerosol aging, Environ. Sci. Technol., 52, 7680-7688, 2018.

Cremer, J. W., Thaler, K. M., Haisch, C., and Signorell, R.: Photoacoustics of single laser-trapped nanodroplets for the direct observation of nanofocusing in aerosol photokinetics, Nature communications, 7, 1-7, 2016.

David, G., Parmentier, E. A., Taurino, I., and Signorell, R.: Tracing the composition of single e-cigarette aerosol droplets in situ by laser-trapping and Raman scattering, Scientific reports, 10, 1-8, 2020.

Esat, K., David, G., Poulkas, T., Shein, M., and Signorell, R.: Phase transition dynamics of single optically trapped aqueous potassium carbonate particles, Physical Chemistry Chemical Physics, 20, 11598-11607, 2018.

Garetz, B. A., Matic, J., and Myerson, A. S.: Polarization switching of crystal structure in the nonphotochemical light-induced nucleation of supersaturated aqueous glycine solutions, Phys. Rev. Lett., 89, 175501, 2002.

Garrison, W. M.: Actions of ionizing radiations on nitrogen compounds in aqueous media, Radiation Research Supplement, 4, 158-174, 1964.

Garrison, W. M.: Radiation-induced reactions of amino acids and peptides, Univ. of California, Berkeley, 1972.

George, C., Ammann, M., D'Anna, B., Donaldson, D., and Nizkorodov, S. A.: Heterogeneous photochemistry in the atmosphere, Chem. Rev., 115, 4218-4258, 2015.

Girod, M., Moyano, E., Campbell, D. I., and Cooks, R. G.: Accelerated bimolecular reactions in microdroplets studied by desorption electrospray ionization mass spectrometry, Chemical Science, 2, 501-510, 2011.

Gong, Z., Pan, Y.-L., Videen, G., and Wang, C.: Optical trapping and manipulation of single particles in air: Principles, technical details, and applications, J. Quant. Spectrosc. Radiat. Transfer, 214, 94-119, 2018.

Hall, J. C.: Glycine, Journal of Parenteral and Enteral Nutrition, 22, 393-398, 1998.

Homchaudhuri, L. and Swaminathan, R.: Near ultraviolet absorption arising from lysine residues in close proximity: a probe to monitor protein unfolding and aggregation in lysine-rich proteins, Bull. Chem. Soc. Jpn., 77, 765-769, 2004.

Jackson, A. A.: The glycine story, Eur J Clin Nutr, 45, 59-65, 1991.

Jawor-Baczynska, A., Moore, B. D., Lee, H. S., McCormick, A. V., and Sefcik, J.: Population and size distribution of solute-rich mesospecies within mesostructured aqueous amino acid solutions, Faraday Discuss., 167, 425-440, 2013.

Kucinski, T. M., Dawson, J. N., and Freedman, M. A.: Size-Dependent Liquid–Liquid Phase Separation in Atmospherically Relevant Complex Systems, The Journal of Physical Chemistry Letters, 10, 6915-6920, 2019.

Lee, J. K., Banerjee, S., Nam, H. G., and Zare, R. N.: Acceleration of reaction in charged microdroplets, Q. Rev. Biophys., 48, 437-444, 2015.

Lee, J. K., Samanta, D., Nam, H. G., and Zare, R. N.: Micrometer-sized water droplets induce spontaneous reduction, Journal of the American Chemical Society, 141, 10585-10589, 2019.

Lundeen, R. A., Janssen, E. M.-L., Chu, C., and McNeill, K.: Environmental photochemistry of amino acids, peptides and proteins, CHIMIA International Journal for Chemistry, 68, 812-817, 2014.

Moenig, J., Chapman, R., and Asmus, K. D.: Effect of the protonation state of the amino group on the. cntdot. OH radical induced decarboxylation of amino acids in aqueous solution, The Journal of Physical Chemistry, 89, 3139-3144, 1985.

Mopper, K. and Zika, R. G.: Natural photosensitizers in sea water: riboflavin and its breakdown products, in, ACS Publications, 1987.

Oraevsky, A. N.: Whispering-gallery waves, Quantum electronics, 32, 377, 2002.

Parmentier, E. A., Corral Arroyo, P., Gruseck, R., Ban, L., David, G., and Signorell, R.: Charge Effects on the Photodegradation of Single Optically Trapped Oleic Acid Aerosol Droplets, The Journal of Physical Chemistry A, 126, 4456-4464, 2022.

Parmentier, E. A., David, G., Arroyo, P. C., Bibawi, S., Esat, K., and Signorell, R.: Photochemistry of single optically trapped oleic acid droplets, J. Aerosol Sci, 151, 105660, 2021.

Pinotsi, D., Buell, A. K., Dobson, C. M., Kaminski Schierle, G. S., and Kaminski, C. F.: A label‐free, quantitative assay of amyloid fibril growth based on intrinsic fluorescence, ChemBioChem, 14, 846-850, 2013.

Pöschl, U. and Shiraiwa, M.: Multiphase chemistry at the atmosphere–biosphere interface influencing climate and public health in the anthropocene, Chem. Rev., 115, 4440-4475, 2015.

Rapf, R. J. and Vaida, V.: Sunlight as an energetic driver in the synthesis of molecules necessary for life, Physical Chemistry Chemical Physics, 18, 20067-20084, 2016.

Reich, O., David, G., Esat, K., and Signorell, R.: Weighing picogram aerosol droplets with an optical balance, Communications Physics, 3, 223, 10.1038/s42005-020-00496-x, 2020.

Ruiz-Lopez, M. F., Francisco, J. S., Martins-Costa, M. T., and Anglada, J. M.: Molecular reactions at aqueous interfaces, Nature Reviews Chemistry, 4, 459-475, 2020.

Shukla, A., Mukherjee, S., Sharma, S., Agrawal, V., Kishan, K. R., and Guptasarma, P.: A novel UV laser-induced visible blue radiation from protein crystals and aggregates: scattering artifacts or fluorescence transitions of peptide electrons delocalized through hydrogen bonding?, Arch. Biochem. Biophys., 428, 144-153, 2004.

Sugiyama, T., Yuyama, K.-i., and Masuhara, H.: Laser trapping chemistry: from polymer assembly to amino acid crystallization, Acc. Chem. Res., 45, 1946-1954, 2012.

Sun, Z., Zhang, C., Xing, L., Zhou, Q., Dong, W., and Hoffmann, M. R.: UV/nitrilotriacetic acid process as a novel strategy for efficient photoreductive degradation of perfluorooctanesulfonate, Environ. Sci. Technol., 52, 2953-2962, 2018.

Swietlicki, E., Hansson, H. C., Hämeri, K., Svenningsson, B., Massling, A., McFiggans, G., McMurry, P. H., Petäjä, T., Tunved, P., Gysel, M., Topping, D., Weingartner, E., Baltensperger, U., Rissler, J., Wiedensohler, A., and Kulmala, M.: Hygroscopic properties of submicrometer atmospheric aerosol particles measured with H-TDMA instruments in various environments—a review, Tellus B: Chemical and Physical Meteorology, 60, 432-469, 10.1111/j.1600-0889.2008.00350.x, 2008.

Tang, I. N., Tridico, A. C., and Fung, K. H.: Thermodynamic and optical properties of sea salt aerosols, Journal of Geophysical Research: Atmospheres, 102, 23269-23275, 10.1029/97jd01806, 1997.

Terpugov, E. L., Kondratyev, M. S., and Degtyareva, O. V.: Light-induced effects in glycine aqueous solution studied by Fourier transform infrared-emission spectroscopy and ultraviolet-visible spectroscopy, J. Biomol. Struct. Dyn., 39, 108-117, 2021.

Tervahattu, H., Tuck, A., and Vaida, V.: Chemistry in prebiotic aerosols: a mechanism for the origin of life, in: Origins, Springer, 153-165, 2004.

Urquidi, O., Brazard, J., LeMessurier, N., Simine, L., and Adachi, T. B.: In situ optical spectroscopy of crystallization: One crystal nucleation at a time, Proceedings of the National Academy of Sciences, 119, e2122990119, 2022.

Walser, M. L., Park, J., Gomez, A. L., Russell, A. R., and Nizkorodov, S. A.: Photochemical aging of secondary organic aerosol particles generated from the oxidation of d-limonene, The Journal of Physical Chemistry A, 111, 1907-1913, 2007.

Wang, X., Gemayel, R., Hayeck, N., Perrier, S., Charbonnel, N., Xu, C., Chen, H., Zhu, C., Zhang, L., and Wang, L.: Atmospheric photosensitization: a new pathway for sulfate formation, Environ. Sci. Technol., 54, 3114-3120, 2020.

Yuyama, K.-i., Sugiyama, T., and Masuhara, H.: Millimeter-scale dense liquid droplet formation and crystallization in glycine solution induced by photon pressure, The Journal of Physical Chemistry Letters, 1, 1321-1325, 2010.

Zaccaro, J., Matic, J., Myerson, A. S., and Garetz, B. A.: Nonphotochemical, laser-induced nucleation of supersaturated aqueous glycine produces unexpected γ-polymorph, Crystal Growth & Design, 1, 5-8, 2001.

Zieger, P., Väisänen, O., Corbin, J. C., Partridge, D. G., Bastelberger, S., Mousavi-Fard, M., Rosati, B., Gysel, M., Krieger, U. K., Leck, C., Nenes, A., Riipinen, I., Virtanen, A., and Salter, M. E.: Revising the hygroscopicity of inorganic sea salt particles, Nature Communications, 8, 15883, 10.1038/ncomms15883, 2017.

Zimbitas, G., Jawor-Baczynska, A., Vesga, M. J., Javid, N., Moore, B. D., Parkinson, J., and Sefcik, J.: Investigation of molecular and mesoscale clusters in undersaturated glycine aqueous solutions, Colloids Surf. Physicochem. Eng. Aspects, 579, 123633, 2019.

419   Figure 1 Counter-propagating tweezers setup. The laser beam is first expanded by a factor of 5 and then split into
420   two beams by the polarizing beam splitter (PBS). The half-waveplate ($\lambda/2$) rotates the polarization to 45° with
421   respect to the axes of the PBS to ensure equal power splitting between the two beams. The beams are aligned on
422   a single axis and focused into the trapping cell using two aspherical lenses (AL). An optical isolator introduced at
423   the start of the beam path prevents unwanted optical feedback into the laser head.

424

425   Figure 2 Setup for TAOS imaging and Raman spectroscopy. The trapping beams run perpendicular to the figure
426   plane. The scattered light of the trapping beams is collected horizontally and vertically at a scattering angle of 90
427   ± 24°. The vertical beam is split into parallel and perpendicular polarized light with respect to the scattering plane
428   and the respective beam is loosely focused on a CMOS camera (P TAOS and S TAOS respectively). The horizontal
429   beam is filtered for the spectral range of 540 – 680 nm and fiber coupled into a low noise, high sensitivity spec-
430   trometer (Spect. Raman) for measurement of the Raman spectrum.

431

432   Figure 3 Analysis of the two-dimensional angular optical scattering spectrum (TAOS). a) Experimental polariza-
433   tion resolved total TAOS signal over time. b) Zoom on a specific time interval for clarity c) Simulated polarization
434   resolved total TAOS signal as function of particle radius in the specific time interval. Arrows indicate the peak
435   assignment based on the similarities between the peak shapes.

436

437   Figure 4 Volume shrinking of glycine droplets as a function of time. a) Droplet trapped at 300 mW nominal laser
438   power b) droplet trapped at 1000 mW nominal laser power c) droplet trapped at 3000 mW nominal laser power.
439   At higher power, the shrinking proceeds faster (visible by the lager slopes). Solid and dashed lines indicate the
440   best linear fit before and after the acceleration of the shrinking observed at approximately a) 280 h, b) 59 h and
441   c) 53 h.

442

443   Figure 5 Fitted shrinking rate as function of light intensity. The solid line indicates the best linear fit through the
444   origin.

445

446   Figure 6 Temporal evolution of Raman signal during droplet shrinking. a) Normalized Raman spectra stacked
447   chronologically from left to right. The molecular Raman bands are visible as horizontal straight white lines on the
448   dark background. The finer, slanted and curved lines correspond to whispering gallery modes. After approximately
449   49 h, the particle leaves the optical trap as it reaches a size that is too small for trapping, and only background is
450   recorded. The band remaining afterwards at 2323 cm^{-1} corresponds to the nitrogen gas in the trapping cell. b)
451   Ratio of the molecular glycine bands centered at 1064 cm^{-1} and 1440 cm^{-1} to the water band at around 3400 cm^{-1}.
452   Peaks and dips in the graphs correspond to spectra where a whispering gallery mode is superimposed on the
453   glycine signal and the water signal, respectively, and are not relevant for the molecular composition. The dashed
454   horizontal lines are a guide to the eye. In this example, the acceleration of the droplet shrinking is observed at t_{acc}

455   = 46 h. From this point in time onwards until the particle is lost, the faster shrinking leads to more frequent WGMs

456   perceived as an apparent increase of noise in the data.

457

458   Figure 7 Acceleration of droplet shrinking versus light intensity. The solid line represents the best linear fit through

459   the measurement data.